Journal of Water Resource and Protection, 2025, 17(12), 842-865
https://www.scirp.org/journal/jwarp
ISSN Online: 1945-3108
ISSN Print: 1945-3094

Assessment of Groundwater Quality in Limbe-Cameroon in a Changing Climate Using a Water Quality Index

Rigobert Motchemien[1*], Charles Bwemba[2], Jean Francois Wounba[2], Gaël Didier Bah Ntutuwouo[3], Valentin Makomra[2], Michel Mbessa[2], George Elambo Nkeng[2], Mathias Fru Fonteh[4]

[1]Department of Rural Engineering, National Advanced School of Public Works Buea, Buea, Cameroon
[2]National Advanced School of Public Works, Yaounde, Cameroon
[3]Institut National de Cartographie, Laboratoire de Gestion des Risques Naturels, Yaounde, Cameroon
[4]Faculty of Agronomy and Agricultural Sciences, The University of Dschang, Dschang, Cameroon
Email: *rmotchemien@gmail.com, matfonteh@yahoo.com

How to cite this paper: Motchemien, R., Bwemba, C., Wounba, J.F., Bah Ntutuwouo, G.D., Makomra, V., Mbessa, M., Nkeng, G.E. and Fonteh, M.F. (2025) Assessment of Groundwater Quality in Limbe-Cameroon in a Changing Climate Using a Water Quality Index. *Journal of Water Resource and Protection*, **17**, 842-865.
https://doi.org/10.4236/jwarp.2025.1712046

Received: October 23, 2025
Accepted: December 19, 2025
Published: December 22, 2025

Abstract

This study assesses the current and future suitability of groundwater in Limbe, Cameroon, for domestic use under the threat of climate change-induced sea level rise. Using physico-chemical analysis, the Revelle Index, and the Water Quality Index (WQI), the authors find that 23% of the groundwater is currently affected by seawater intrusion. Projections indicate that this will increase to 30.8% by 2050 and 42.31% by 2100, significantly reducing the proportion of water that is safe for drinking.

Keywords

Climate Change, Sea Level Rise, Seawater Intrusion, Pollution, Revelle Index

1. Introduction

In the last few decades, there has been a tremendous increase in the demand for fresh water due to the rapid growth of the population and the accelerated pace of industrialization [1]. Human health is threatened by climate change and also by excessive application of fertilizers and unsanitary conditions [2]. Limbe, a coastal city in Cameroon on the Atlantic Ocean, has a demand for domestic water supply that the water utility company cannot satisfy, and hence a significant proportion of the population relies on groundwater (gw) to meet their domestic water demands. In the study area, about 250 wells have been abandoned because the water

has become salty, probably due to sea water intrusion [3].

Under natural conditions, coastal aquifers are recharged by rainfall, and the gw flows towards the ocean, preventing saltwater from encroaching into the freshwater region. The global mean sea level (GMSL) increased by an average rate of 1.8 mm/year during the 20th century [4] and the [5] reported with high confidence that this rate has been increasing [6]. The IPCC estimated that the GMSL increased by 3.1 mm/year from 1993 to 2003, although this change is not spatially uniform worldwide. [7] estimated a GMSL rise of approximately 3.3 mm/year in the period 1992 to 2010.

[3] estimated on the basis of data obtained from the tide gauge installed in Limbe, a rise in the level of the ocean in the lower part of the Gulf of Guinea of about 10 mm/year. One effect of such an increase in sea level is to induce seawater intrusion into coastal aquifers [8]. This saltwater intrusion is a serious environmental issue since 80% of the world's population lives along the coast and utilizes local aquifers for their water supply. In addition, overexploitation of coastal aquifers has resulted in reduced groundwater levels (hence reduced natural flow), and this has led to severe saltwater intrusion. Cases of saltwater intrusion, with varying degrees of severity and complexity, have been documented throughout the Atlantic coastal zone. For example, in New Jersey, more than 120 wells have been abandoned because of saltwater contamination [9].

Researchers have also reported that variations in sea level and the associated wedge movement can influence near-shore and/or large-scale submarine discharge patterns and impact nutrient loading levels across the aquifer-ocean interface [10]. While anthropogenic activities, such as overpumping and felling of trees in urbanized coastal areas, are the major causes of saltwater intrusion, it is projected that increases in sea level due to climate change would aggravate the problem [10]. [11] modelled the impacts of climate change and changes in land use patterns on the salt distribution in a coastal aquifer and concluded that rising sea level could induce rapid progression of saltwater intrusion.

Excessive groundwater withdrawals have been reported to result in hydrochemical changes in the physical, chemical, and microbiological water quality, a decline of the water table, reverse hydraulic gradient, and consequently, water quality deterioration in coastal areas [12]. Poor water quality results in incidences of waterborne diseases and consequently reduces the life expectancy of the population [13]. Thus, concern for clean and safe drinking water and protection from contamination is justified because a large proportion of the population in the study area depends on wells and boreholes for domestic purposes.

Water quality evaluation is based on the physical, chemical, and biological parameters ascertaining the suitability for various uses such as domestic consumption, agricultural, recreational, and industrial use [14]. The traditional assessment of water quality consists of comparing the point values of water quality parameter levels with their guideline or standard values based on allocated water use or uses. This type of assessment does not provide an overall assessment of the water qual-

ity of a water body, which is important for managers and decision-makers. To resolve this decision-making problem, several water quality indices have been developed to transform water quality parameter levels into an integrated indicator value. Many studies have been carried out to assess the gw quality using the WQI. For instance, [15] compared groundwater quality in Gandhinagar Taluka in India and developed the water quality index for the area. [16] classified salinization of groundwater in the shallow aquifer of a small tropical island in Sabah, Malaysia using the Revelle index. [17] also adopted this index to evaluate seawater intrusion into the coastal aquifer in India.

[18] Evaluating the groundwater salinization proved that 56.9% of the samples are unaffected, 41.4% are slightly influenced, and 1.7% of groundwater was strongly affected. This infers that fresh groundwater contamination by salinity is a major concern for the freshwater supply in the study area, especially around locations 21, 25 - 30, 33 - 37, 41 - 44, and 51 - 58. Thus, there is a need to regulate groundwater exploitation through monitoring by concerned agencies for sustainable groundwater resource management. The suitability of groundwater for drinking purposes shows that about 37.9% of the samples had excellent water quality, and 48.3%, 12.1%, and 1.7% indicate good, poor, and water unfit for drinking, respectively. It is deduced that locations around 9 - 10, 16 - 17, 21, and 28 pose a great threat to water quality in the study area. However, the study concluded that the water quality of the study area is of good quality, since about 86.2% is suitable for drinking purposes.

[19] used the WQI to assess the groundwater quality of Malda district, West Bengal, in India. The study showed that the range of WQI values was 68.32 to 621.03; "very poor" and "water unsuitable for drinking" accounted for 26% and 17%, respectively, of the analyzed groundwater samples. These two water categories contained a high concentration of heavy metals, such as Cu, Cd, Mn, Fe, Cr, and As. The quality of groundwater of Tumkur Taluk, Karnataka State, was examined by [20] using the WQI. The study revealed that the WQI ranged from 89.21 to 660.56. The high value of WQI was caused by higher contents of Fe, NO_3, TDS, hardness, F, HCO_3, and Mn in groundwater. The assessment of groundwater quality in Thirumanimuttar sub-basin, Tamil Nadu, by [19] found WQI values ranging from 37.94 to 298.96 and 41.35 to 291.94 for pre- and post-monsoon seasons, respectively. The pre-monsoon samples exhibited a greater percentage of poor quality compared to post-monsoon samples. [21] applied WQI in the assessment of groundwater quality for human consumption in Visakhapatnam City, Andhra Pradesh. The investigation recorded WQI values in the range of 28 to 267. The study found that 16%, 14%, and 12% of groundwater samples pertaining to pre-monsoon, monsoon, and post-monsoon seasons were of "poor quality"; and 2%, 6%, and 4% of groundwater samples during these seasons, respectively, were of "very poor quality". The study concluded that "poor quality" was attributed to high contents of TDS, NO_3, and Cl; and "very poor quality" was because of high values of hardness, Ca, Mg, Cl, NO_3, and TDS. According to [22], the water quality

index (WQI) ranged from 15.27 to 550.97 mg/l. The spatial variations in the samples revealed that about 37.9% of the sampled wells had excellent water quality and 48.3%, 12.1% and 1.7% indicated good, poor, and water unfit for drinking, respectively. All of these studies proved the usefulness of the WQI method in the assessment of drinking water quality.

The aim of this study was to determine the suitability of the gw in Limbe for domestic use in a changing climate. The specific objectives were to determine if sea water is polluting the gw in Limbe; assess the current spatial variability of the gw quality using a WQI; and finally, determine the spatial variability of water quality due to sea level rise resulting from climate change.

2. Materials and Methods

2.1. Study Area

2.1.1. Location

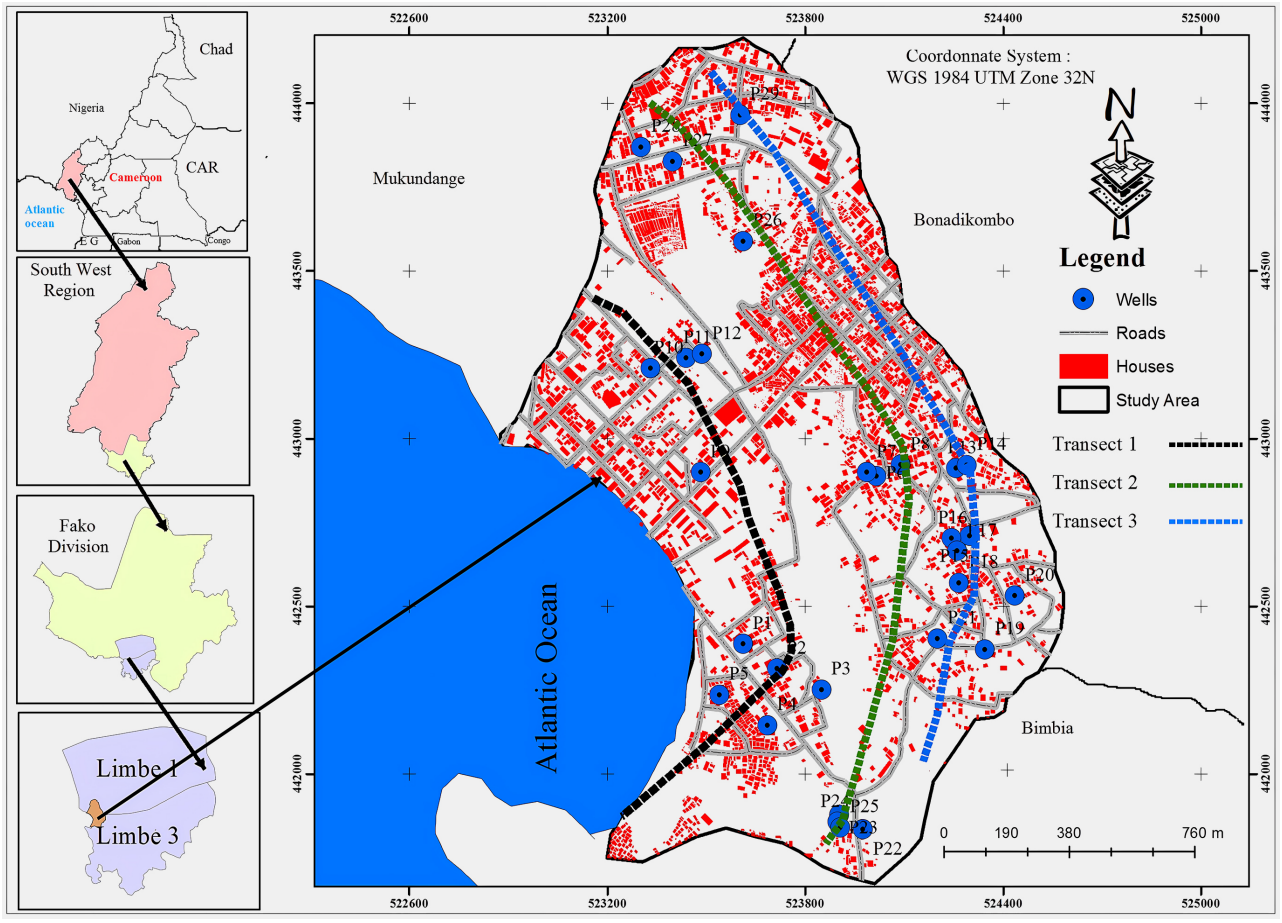

Figure 1. Study location and sample collection points.

The city of Limbe is located along the coastal area of Fako Division, South-West Region of Cameroon (Figure 1). The study area is located approximately between latitudes 3˚90' and 4˚05'N and longitudes 9˚29' and 9˚06'E. It is bounded in the

east by Bimbia, in the north by Bonadikombo, in the south by the Atlantic Ocean and in the west by Mukundange. The population of Limbe was estimated at 130,000 inhabitants spread over a surface area of 596 km^2, giving a population density of 218 persons/km^2 [23].

The city is characterized by a low-lying coastal plain, rising to a chain of horse-shoe-shaped hills towards the northeast and east, with the highest points reaching 362 m above sea level [24]. Within the city, small streams flow into larger drainage channels that converge into the main river (Njenguele) that empties into the Atlantic Ocean (**Figure 2**). These rivers frequently overflow their banks in the rainy season, causing floods in the low-lying areas that are only 1 - 2 m above sea level [25]. The hills that surround the city are made up of loose ferralitic and volcanic soils that easily disintegrate when they absorb a lot of water [26].

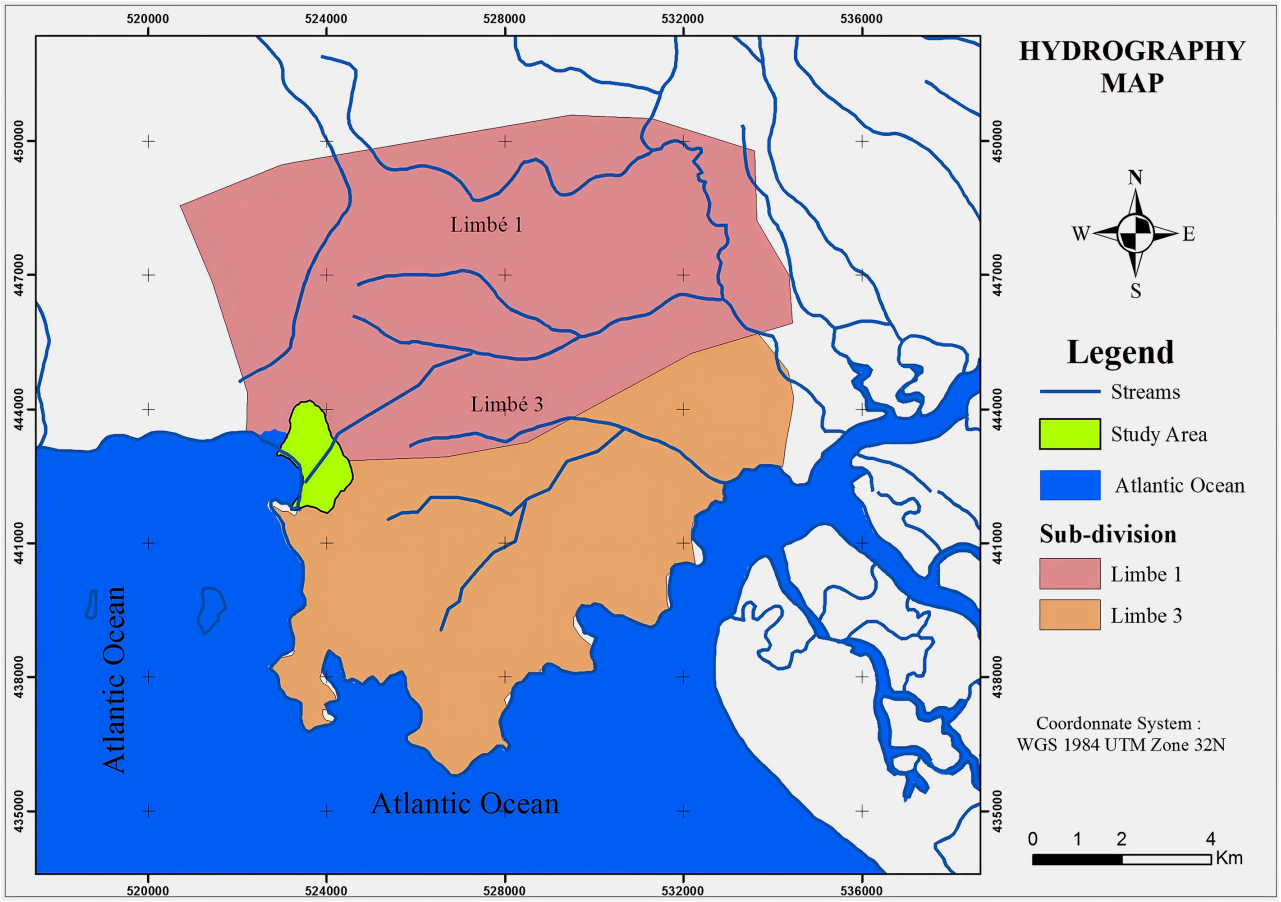

Figure 2. Hydrography of the study area. Source: [27].

2.1.2. Climate

The climate of Limbe is of the subequatorial type with two distinct seasons: a two-month dry season from December to January and a 10-month rainy season that runs from February to November, with a mean annual rainfall of about 3100 mm, ±1100 standard deviation [28]. The peak rainfall is recorded from June to August and sometimes in September. The monthly rainfall frequently exceeds 500 mm

and is sometimes over 1000 mm in June, July, and August. The mean annual temperature is about 26˚C, while the relative humidity is generally above 85% [29].

2.1.3. Geomorphology and Hydrogeology

Geomorphologically, the study area is made up of ridges and deeply incised ravines with a W-E orientation at a high angle to the general NE-SW orientation of Mount Cameroon [28]. The elevations in the study area range from 0 m to about 90 m above sea level, with slopes ranging from 0˚ to 43˚ (**Figure 3**). The slopes at the foot of Mount Cameroon are composed of multiple porphyritic basaltic lava flows, punctuated by several strombolian pyroclastic cones to the W and NW and lahar deposit to the E of the study area [30]. These ridges form part of the Limbe-Mabeta Volcanic Massif, made up of degraded and deeply weathered tertiary basaltic lava flows [28]. The main rock types within this area include basalts, basanites, lahar deposits, and pyroclastic materials [27].

The hydrogeology is characterized by unfossiliferous sandstone and gravel weathered from underlying Precambrian basement rock [31]. It consists of Coastal Plain Sands (CPS) and recent sediments. The CPS aquifer is the most productive and exploited aquifer in Limbe.

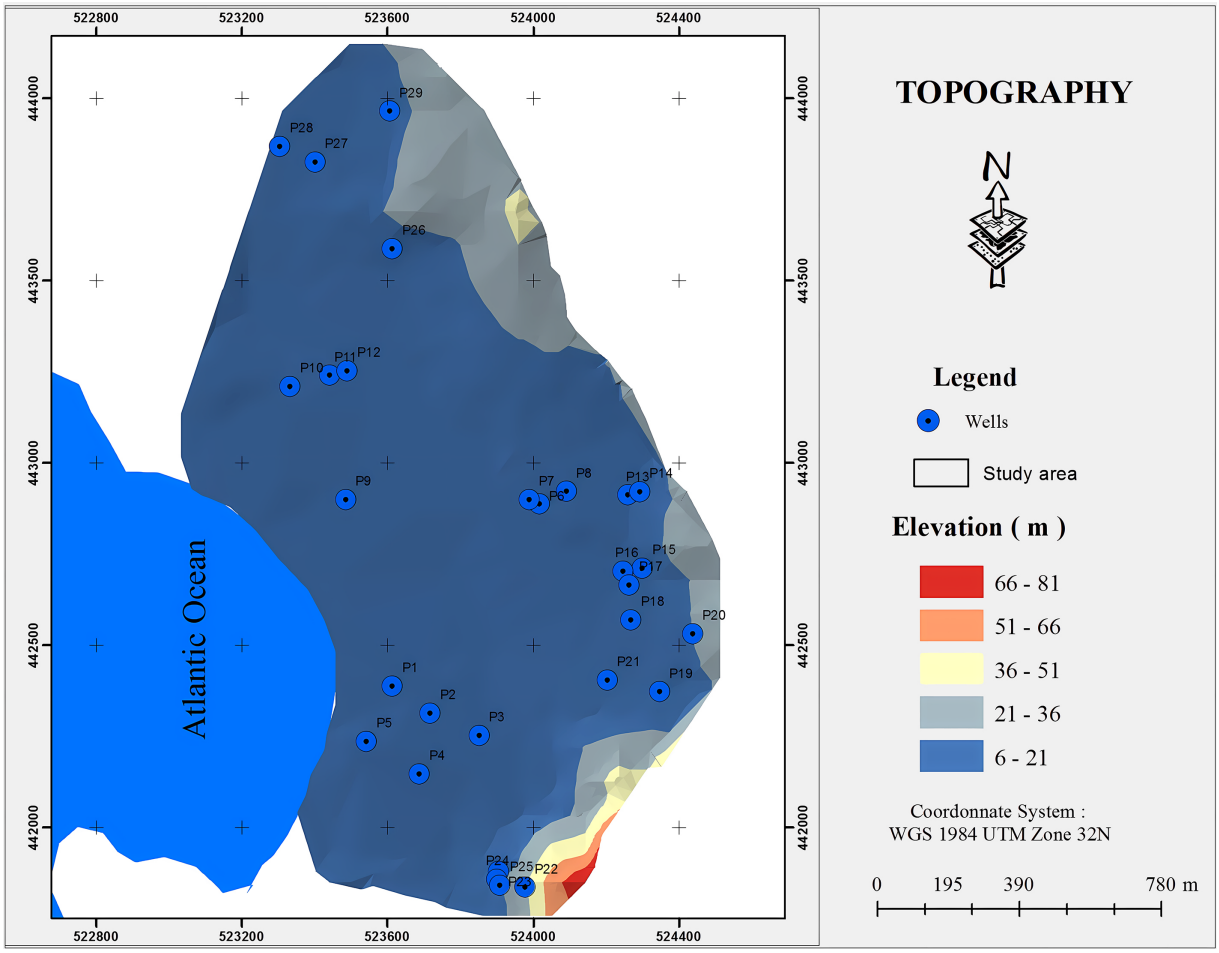

Figure 3. Topographic map of the study area.

2.2. Data

2.2.1. Assessment of the Pollution of Gw by Seawater Intrusion

Water samples were collected monthly between July 2017 and June 2018 from thirty hand-dug wells located along three transects (T_1, T_2, T_3) for evaluation of groundwater salinization and water quality assessment (**Figure 1**). The size of the sample required from the target population was determined according to the formula presented in Equations (1) and (2) [32]:

$$m = \frac{z^2}{\varepsilon^2} p(1-p) \tag{1}$$

$$n = \frac{m}{1+\frac{m-1}{N}} \tag{2}$$

where:

- m is the sample size.
- n is the corrected sample size for a limited population.
- N is the population.
- Z is the value related to the confidence level (1.96 for 95% confidence level).
- P is the degree of variance between the elements of the population (0.5).
- ε is the maximum error (0.07).

The electrical conductivity (EC), the pH, and the total dissolved solids (TDS) were measured in situ using a portable handheld pH-028 six-in-one monitor. Water samples for laboratory analysis were collected in clean 150 ml polyethylene bottles and preserved in ice chests for analyses of chloride and bicarbonate using standard methods [33]. Coordinates of the sampled wells were recorded using a Global Positioning System (GPS) and were thereafter plotted using ArcGIS software on the geomorphological map of Limbe.

The evaluation of groundwater pollution from seawater intrusion was assessed using the Revelle Index [34], given by:

$$\mathrm{RI} = \frac{\left[\mathrm{Cl}^-\right]}{\left[\mathrm{HCO}_3^-\right]+\left[\mathrm{CO}_3^{2-}\right]} \tag{3}$$

where:

- RI is the Revelle Index.
- $\left[\mathrm{Cl}^-\right]$ is the concentration of chloride in the sample.
- $\left[\mathrm{HCO}_3^-\right]$ is the concentration of bicarbonate in the sample.
- $\left[\mathrm{CO}_3^{2-}\right]$ is the concentration of carbonate in the sample.

According to [34], when RI < 0.5, this indicates the water has not been affected by groundwater intrusion; when RI is between 0.5 - 6.6, this indicates it is lightly affected, and when it is greater than 6.6, it indicates it is strongly affected.

2.2.2. The Current Spatial Variability (SP) and SP of Water Quality Due to Sea Level Rise Resulting from Climate Change Using WQI

The drinking water quality was assessed using a water quality index (WQI) and the [13] standard. The stages of calculating the WQI are as follows:

$$q_n = 100\frac{V_n - V_{io}}{S_n - V_n} \tag{4}$$

where:

- q_n = quality rating for the n^{th} water quality parameter.
- n = the water quality parameter and quality rating or sub-index (q_n) corresponding to n^{th} parameter, *i.e.*, a number reflecting the relative value of this parameter with respect to its standard (maximum permissible value).
- V_n = estimated value of the n^{th} parameter at a given sampling point.
- S_n = standard permissible value of the nth parameter.
- V_{io} = ideal value of the n^{th} parameter in pure water, *i.e.*, 0 for all other parameters except pH and dissolved oxygen (7.0 and 14.6 mg/l, respectively).

The unit weight of the n^{th} parameter (W_n) was calculated by a value inversely proportional to the recommended standard value (S_n) of the corresponding parameter.

$$W_n = \frac{K}{S_n} \tag{5}$$

where:

- S_n = standard value for the n^{th} parameter.
- K = constant of proportionality ($K = \frac{1}{\sum\left(\frac{1}{S_n}\right)}$).

The WQI was then calculated using Equation (6):

$$\text{WQI} = \frac{\sum q_n W_n}{\sum W_n} \tag{6}$$

Table 1 shows the classification of water based on the WQI, from the point of potability.

Table 1. Water Quality Index (WQI) and status of water quality.

Water Quality Index Level	Water Quality Status
0 - 25	Excellent water quality
26 - 50	Good water quality
51 - 75	Poor water quality
76 - 100	Very poor water quality
Above 100	Unsuitable for drinking

Source: [36].

The coordinates of each sample were determined using a Garmin GPSmap 78S. The computed Revelle and WQIs were then exported to the ArcGIS 6.0 software package to generate maps that include information relating to the Revelle index,

water quality index and its distribution over the study area.

Finally, slicing options were applied using these ranges of values with five groups of water quality classes to generate a spatial distribution of the water quality map [35]. The statistical analysis of the examined groundwater parameters was computed using STATA software version 6.0.

The effect of CC on seawater intrusion in the study area was determined using the estimation of the SLR; the determination of the retreat in the shoreline; the hydraulic head of the coastal aquifer due to CC, and the velocity of the gw. Reference [3] showed that there was a correlation between sea level and the temperature of ocean surface waters at Limbe in Cameroon. This study noted the increase in sea level at the Limbe coasts of 10 mm/year and a retreat in the shoreline of 32 cm/year. This recession will leave a space favorable to saline intrusion, the consequence of which will be the advancement of the saltwater front. The projection of the sea level rise for 2050 and 2100 was obtained by using (7) and (8), respectively.

$$\text{SLR2050} = \text{annual rate of SLR} \times (2050 - 2018) \tag{7}$$

$$\text{SLR2100} = \text{annual rate of SLR} \times (2100 - 2018) \tag{8}$$

The projected retreat or recession in the shoreline in 2050 and 2100 was obtained using (9) and (10), respectively.

$$\begin{aligned}&\text{Retreat in the shoreline in 2050}\\&= \text{annual retreat in the shoreline rate} \times (2050 - 2018)\end{aligned} \tag{9}$$

$$\begin{aligned}&\text{Retreat in the shoreline in 2100}\\&= \text{annual retreat in the shoreline rate} \times (2100 - 2018)\end{aligned} \tag{10}$$

The velocity of flow of the gw in 2018 was obtained using Darcy's formula in (11):

$$v = Ki \tag{11}$$

where:

- v = velocity of flow of the gw (cm/s).
- K = soil permeability (cm/s).
- i = hydraulic gradient (ratio).

The soil permeability was obtained using the Porchet method. For this, a cylindrical hole was dug with an auger 10 cm in diameter and 50 cm deep. After filling the hole with water, the height of the water h_1 was noted at time t_1 and later h_2 at time t_2.

The permeability of the soil K was obtained from (12)

$$K = \frac{r}{2(t_2 - t_1)} \ln \frac{h_1 + \frac{r}{2}}{h_2 + \frac{r}{2}} \tag{12}$$

where:

- K = soil permeability (cm/s).
- r = radius of the hole (cm).

- h_1 = height of the water (cm) at time t_1 (s).
- h_2 = height of the water (cm) at time t_2 (s).

In a free porous type aquifer, the dominant flows are horizontal, as a consequence of a weak hydraulic gradient in low-lying areas [36]. The piezometric level is influenced by the geometry, the topography, the hydrodynamic properties of the soil, and the operating conditions. From the base year of 2018, wells that had been affected by salt intrusion were retained because their hydraulic heads were greater than those of the other wells. The salty well (P_3) with the highest hydraulic head and the well (P_9) with the lowest hydraulic head were used for the estimation of the hydraulic gradient.

The hydraulic gradient of the aquifer water was determined using (13):

$$i = \frac{dH}{dL} \tag{13}$$

where:

- i = hydraulic gradient (ratio).
- dh = the difference in head compared to an upstream well and a downstream well (m).
- dl = the distance between the two wells (m).

The salt front was measured from the coastline using the "distance measurement" application in ArcGIS software. As the sea level rose, this front had to move from the highest hydraulic head to the lowest due to the increased hydraulic head in the wells in the critical zone. The simulation of [36] gives the hydraulic head in the coastal aquifer equal to half the rise in sea level during this period, and this was used in the study. The salt front during displacement affected new wells (P_6, P_7, P_{10}) with concentrations equal to those of wells from the initial position of the salt front. These new concentrations were substituted with the old concentrations from which the Revelle indices (RI) for 2050 and 2100 (only well P_8 was affected and P_{10} excluded) were calculated according to the formulas of (14) and (15):

$$\mathrm{RI}_{2050} = \frac{\left[\mathrm{Cl}^-\right]_{2050}}{\left[\mathrm{HCO}_3^-\right] + \left[\mathrm{CO}_3^{2-}\right]} \tag{14}$$

$$\mathrm{RI}_{2100} = \frac{\left[\mathrm{Cl}^-\right]_{2100}}{\left[\mathrm{HCO}_3^-\right] + \left[\mathrm{CO}_3^{2-}\right]} \tag{15}$$

For the projections with rising sea levels due to climate change, the hydraulic gradients for the years 2050 and 2100 were estimated based on the (16) and (17). The new velocity of the salt fronts for these respective years was obtained with the (18) and (19), and finally the projected displacement of the salty front was obtained with (20) and (21), respectively, for 2050 and 2100.

$$i_{2050} = \frac{dh_{2050}}{dl} \tag{16}$$

$$i_{2100} = \frac{dh_{2100}}{dl} \tag{17}$$

$$v_{2050} = Ki_{2050} \tag{18}$$

$$v_{2100} = Ki_{2100} \tag{19}$$

$$d_{2050} = v_{2050}t_{50} \tag{20}$$

$$d_{2100} = v_{2100}t_{100} \tag{21}$$

where:

- i_{2050} and i_{2100} are the hydraulic gradients in 2050 and 2100, respectively.
- dh_{2050} and dh_{2100} are the differences in load compared to an upstream well and a downstream well in 2050 and 2100, respectively (m).
- dl = the distance between the two wells (m).
- v_{2050} and v_{2100} are the velocities of gw in 2050 and 2100, respectively (cm/s).
- K is the soil permeability (cm/s).
- d_{2050} and d_{2100} are the displacements of the salt front in 2050 and 2100, respectively (m).
- t_{50} = 2050 − 2018 = 32 years.
- t_{100} = 2100 − 2050 = 50 years.

As the hydraulic gradient will change with the sea level, the impact will be on the concentration of chloride. WQI for the years 2050 and 2100 was obtained with (22) and (23), respectively.

$$\mathrm{WQI}_{2050} = \frac{q_{\mathrm{pH}}W_{\mathrm{pH}} + q_{\mathrm{TDS}}W_{\mathrm{TDS}} + q_{\mathrm{EC}}W_{\mathrm{EC}} + q_{\left[\mathrm{Cl}^-\right]_{2050}}W_{\left[\mathrm{Cl}^-\right]_{2050}} + q_{\left[\mathrm{HCO}_3^-\right]}W_{\left[\mathrm{HCO}_3^-\right]}}{W_{\mathrm{pH}} + W_{\mathrm{TDS}} + W_{\mathrm{EC}} + W_{\left[\mathrm{Cl}^-\right]_{2050}} + W_{\left[\mathrm{HCO}_3^-\right]}} \tag{22}$$

$$\mathrm{WQI}_{2100} = \frac{q_{\mathrm{pH}}W_{\mathrm{pH}} + q_{\mathrm{TDS}}W_{\mathrm{TDS}} + q_{\mathrm{EC}}W_{\mathrm{EC}} + q_{\left[\mathrm{Cl}^-\right]_{2100}}W_{\left[\mathrm{Cl}^-\right]_{2100}} + q_{\left[\mathrm{HCO}_3^-\right]}W_{\left[\mathrm{HCO}_3^-\right]}}{W_{\mathrm{pH}} + W_{\mathrm{TDS}} + W_{\mathrm{EC}} + W_{\left[\mathrm{Cl}^-\right]_{2100}} + W_{\left[\mathrm{HCO}_3^-\right]}} \tag{23}$$

where

- q_{pH} = quality rating for the pH.
- q_{TDS} = quality rating for the TSD.
- q_{EC} = quality rating for the CE.
- $q_{\left[\mathrm{Cl}^-\right]_{2050}}$ = quality rating for chloride in 2050.
- $q_{\left[\mathrm{HCO}_3^-\right]}$ = quality rating for the bicarbonate.
- $q_{\left[\mathrm{Cl}^-\right]_{2100}}$ = quality rating for chloride in 2100.
- W_{pH} = unit weight for the pH.
- W_{TDS} = unit weight for the TDS.
- W_{EC} = unit weight for the EC.
- $W_{\left[\mathrm{Cl}^-\right]_{2050}}$ = unit weight of chloride in 2050.
- $W_{\left[\mathrm{Cl}^-\right]_{2100}}$ = unit weight of the chloride in 2100.
- $W_{\left[\mathrm{HCO}_3^-\right]}$ = unit weight for the bicarbonate.
- WQI_{2050} and WQI_{2100} were imported into the software ArcGIS for digitizing

maps. The areas occupied by the various water quality classes were obtained after circumscribing each color with the "surface" application of the software.

3. Results and Discussion

3.1. Pollution of Gw by Seawater Intrusion

Table 2 gives the measured parameters in the three transects as well as the descriptive statistics of the physical and chemical parameters of groundwater samples in the study area. These results were compared with the standard guideline values recommended by the World Health Organization.

Table 2. Measured parameters and descriptive statistics of groundwater in the study area.

Transect	Wells	EC (µS/cm)	pH	TDS (ppm)	T (˚C)	$[Cl^-]$ (mg/l)	$[HCO_3^-]$ (mg/L)	$[Cl^-]/[HCO_3^-]$
T1	P1	592.92	7.19	419.17	28.09	93.21	85.6	1.09
T1	P2	794.17	7.05	558.33	27.89	112.13	82.7	1.36
T1	P3	680	7.26	475.83	27.77	90.29	88.71	1.02
T1	P4	808.33	7.34	566.67	26.88	131.63	105.38	1.25
T1	P5	792.5	7.24	555	27.04	140.4	90.53	1.55
T1	P9	497.27	6.86	340	27.83	65.52	83.47	0.78
T1	P10	451.67	7.26	317.5	27.48	77.42	75	1.03
T1	P11	570.83	6.99	399.17	27.83	74.1	90.43	0.82
T2	P6	494	7.2	331.67	26.57	88.53	124.94	0.71
T2	P7	655	7.49	429.17	27.28	83.27	196.83	0.42
T2	P8	698	7.09	455	27.2	102.77	160.81	0.64
T2	P12	519	7.22	340	27.63	39.59	120.82	0.33
T2	P15	120	6.46	82.5	27.58	34.13	137.96	0.25
T2	P16	145	6.58	100	27.98	39	107.4	0.36
T2	P17	195	6.66	143.33	27.31	25.94	107.8	0.24
T2	P18	400	6.99	271.67	27.81	39	109.6	0.36
T2	P19	121	6.74	85	27.67	43.68	128.83	0.34
T2	P21	254	6.64	176.67	27.48	39	109.3	0.36
T2	P26	287	6.94	214.17	26.88	40.95	79.5	0.52
T2	P27	452	7.31	316.67	27.7	23.4	103.41	0.23

Continued

T2	P28	369	7.12	252.5	27.78	22.43	101.77	0.22
T2	P29	249	6.63	185.83	27.91	25.35	105.36	0.24
T2	P30	327.27	6.96	240	27.48	24.38	105.86	0.23
T3	P13	298	7.37	189.17	27.23	25.35	170.7	0.15
T3	P14	262	6.34	185	27.5	30.81	128.2	0.24
T3	P20	233	6.2	160.83	27.75	50.12	126.98	0.39
T3	P22	203	6.79	143.33	27.73	41.93	185.95	0.23
T3	P23	222	6.85	153.33	27.03	33.15	159.62	0.21
T3	P24	230	6.84	159.17	27.88	41.73	193.57	0.22
T3	P25	232	6.71	156.67	27.2	59.09	184.32	0.32
	Min	**120**	**6.2**	**82.5**	**26.57**	**22.43**	**75**	**0.15**
	Max	**808.33**	**7.49**	**566.67**	**28.09**	**140.4**	**196.83**	**1.55**
	Mean	**405.1**	**6.94**	**280.11**	**27.51**	**57.94**	**121.71**	**0.54**
	Standard dev	**213.61**	**0.32**	**146.58**	**0.38**	**33.67**	**36.26**	**0.39**
	WHO norm	**300**	**6.5 - 8.5**	**500**	**25**	**250**	**300**	

Where min = minimum; max = maximum; EC = Electrical Conductivity; and TDS = Total Dissolved Solids.

The pH of the sampled wells varied from 6.2 to 7.49 with a mean value of 6.94, indicating the nearly neutral condition of the groundwater. The EC values varied from 120.00 µS/cm to 808.33 µS/cm with a mean value of 405.10 µS/cm. The values of EC in all wells in transect 1 exceeded the minimum recommended value. The total dissolved solids ranged from 82.50 ppm to 566.67 ppm with a mean value of 280.11 mg/l. In natural water, dissolved solids are composed mainly of carbonates, bicarbonates, chlorides, sulphates, phosphates, nitrates, calcium, magnesium, sodium, potassium, iron, and manganese [37]. They originate from the dissolution or weathering of the rocks and soil, including dissolution of lime, gypsum, and other slowly dissolved soil minerals. Most of the values of the TDS were within the recommended range for drinking water except for values obtained from wells P_2, P_4 and P_5, which exceeded the recommended value. The temperature varied between 26.57˚C and 28.09˚C with a mean value of 27.51. These values are above the WHO recommended values. This was due to the fact that the ambient temperature greatly affected the groundwater temperature since most of the wells were shallow. The bicarbonate level varied between 75.00 and 196.83 mg/l with a mean value of 121.71 mg/l. Chloride values were found to vary from 22.43 to 140.4 mg/l with a mean value of 57.94. These values of chloride are within the recommended standard level. A high level of chloride in freshwater is an indicator of

pollution [37]. The Secondary Maximum Contaminant Limit (SMCL) for chloride is 250 mg/l. This is the level above which the taste of the water may become objectionable to the consumer. In addition to the adverse taste effects, high chloride concentration levels in the water contribute to the deterioration of domestic plumbing, water heaters, and equipment in municipal water works. High chloride concentrations in the water may also be associated with the presence of sodium in drinking water. The levels of TDS, EC, and Cl^- decreased significantly from transect 1 to 3 as shown in **Table 3**, while the level of bicarbonate ions rather increased significantly. This indicated that saline intrusion was more pronounced in sites near the ocean.

Table 3. Spatial variation of analyzed parameters according to transects.

Transect	Temp (˚C)	pH	TDS (ppm)	EC (µS/cm)	$[Cl^-]$ (mg/l)	$\left[HCO_3^-\right]$ (mg/L)	Cl^-/HCO_3^-
T_1	27.60^a	7.15^b	453.96^{c**}	648.46^{c**}	98.09^{c**}	87.73^{a**}	1.11^{c**}
T_2	27.48^a	6.93^b	241.61^{b**}	352.35^{b**}	44.76^{b**}	120.01^{b**}	0.36^{b**}
T_3	27.47^a	6.73^{a*}	163.93^{a**}	240.00^{a**}	40.31^{a**}	164.19^{c**}	0.25^{a**}

TDS (Total Dissolved Solids), EC (Electrical Conductivity); No significant difference exists in the columns for the values carrying the same letters ($p > 0.05$); Significant differences in the columns for the values carrying different letters ($^*p < 0.05$; $^{**}p < 0.001$).

In the study area, RI varied from 0.126 and 1.551 as shown in **Table 4**. This suggests that some areas in the study area have not been affected while others have been slightly affected. The relationship between the ratios of $Cl/HCO_3 + CO_3$ indicates a strong positive linear relation with Cl concentrations ($r = 0.94$, $p < 0.01$). This linear relationship indicates the mixing of saline water and fresh groundwater [16]. **Figure 4** shows the spatial variation of the extent of groundwater salinization in the study area. About 77% of the groundwater in the study area was unaffected by seawater intrusion, while 23% of the aquifer was slightly affected by pollution from seawater. The hotspots include locations of wells P_1, P_2, P_3, P_4, P_5. Thus, effort must be made to reduce the pollution of groundwater due to sea level rise in the area.

Table 4. Revelle Index of gw in the study area.

Transects	Wells	X	Y	Revelle index 2018	Revelle index 2050	Revelle index 2100
T1	P1	523,612	442,388	1.089	1.089	1.089
T1	P2	523,716	442,314	1.356	1.356	1.356
T1	P3	523,850	442,252	1.018	1.018	1.018
T1	P4	523,686	442,146	1.249	1.249	1.249

Continued

T1	P5	523,541	442,236	1.551	1.551	1.551
T1	P9	523,484	442,900	1.061	1.061	1.061
T1	P10	523,331	443,210	1.11	1.11	1.11
T1	P11	523,439	443,241	1.136	1.136	1.136
T2	P6	524,016	442,888	0.524	0.746	0.746
T2	P7	523,988	442,900	0.393	0.57	0.57
T2	P8	524,090	442,922	0.461	0.561	0.561
T2	P12	523,488	443,253	0.328	1.089	1.089
T2	P15	524,299	442,711	0.184	0.184	1.018
T2	P16	524,245	442,703	0.287	0.287	0.824
T2	P17	524,262	442,665	0.317	0.317	0.772
T2	P18	524,267	442,570	0.356	0.356	0.356
T2	P19	524,346	442,372	0.201	0.201	0.201
T2	P21	524,202	442,404	0.357	0.357	0.357
T2	P26	523,612	443,589	0.549	0.549	0.549
T2	P27	523,399	443,827	0.485	0.485	0.485
T2	P28	523,303	443,870	0.383	0.383	0.383
T2	P29	523,604	443,966	0.398	0.398	0.398
T2	P30	523,634	443,866	0.313	0.313	0.313
T3	P13	524,259	442,912	0.244	0.244	0.244
T3	P14	524,291	442,921	0.461	0.461	0.461
T3	P20	524,437	442,532	0.322	0.322	0.322
T3	P22	523,976	441,835	0.126	0.126	0.126
T3	P23	523,903	441,878	0.140	0.14	0.14
T3	P24	523,899	441,857	0.131	0.131	0.131
T3	P25	523,907	441,841	0.132	0.132	0.132
			Min	**0.126**	**0.126**	**0.126**
			Max	**1.551**	**1.551**	**1.551**
			Mean	**0.555**	**0.597**	**0.658**
			Standard devia	**0.418**	**0.425**	**0.417**

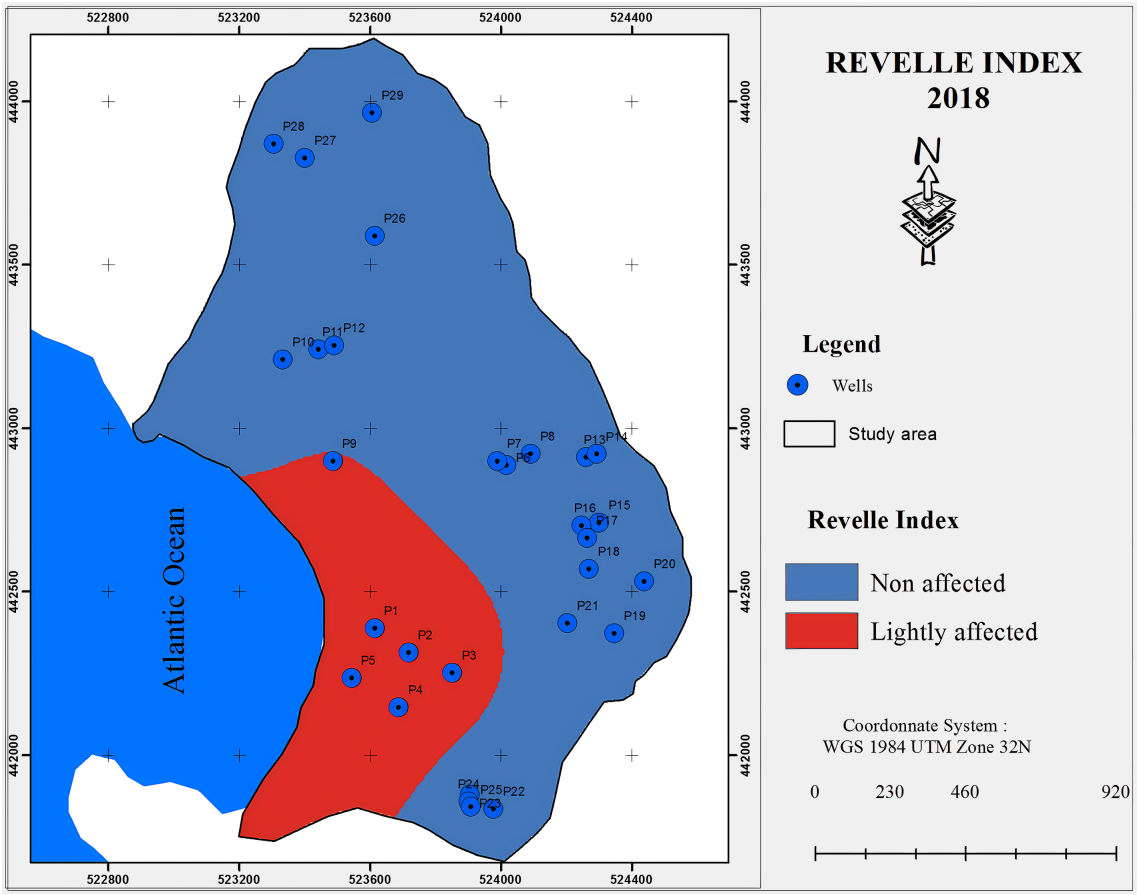

Figure 4. Spatial variation of Revelle index 2018.

With the projected sea level rise (SLR) of 32 cm in 2050 and 82 cm in 2100 due to climate change, the hydraulic head will be increased in the critical wells by 0.16 m in 2050 and 0.492 m in 2100, based on simulations by [38]. A negative hydraulic gradient will result and will lead to a change in the RI. **Figure 5** and **Figure 6** show the spatial variations of RI in 2050 and 2100, respectively, as influenced by projected sea level rise. The area covered by various RI values was calculated from the RI maps and is presented in **Table 5**. The area lightly affected will increase from 55.36 ha in 2018 to 74.32 ha in 2050, leading to an increment of 7.8% of the total area lightly affected. The increment will be 11.51% by 2100. The model assumes that, as the saltwater front advances, newly affected wells adopt the exact chemical concentrations of wells at the front's initial position, which can be a limitation of the study.

Table 5. Areas affected by chloride ions according to the Revelle Index.

	2018 (ha)	2050 (ha)	2100 (ha)
Not affected by chlorides	185.96 (77%)	167 (69.20%)	139.21 (57.69%)
Lightly affected by chlorides	55.36 (23%)	74.32 (30.8%)	102.11 (42.31%)
Total	241.32 (100%)	241.32 (100%)	241.32 (100%)

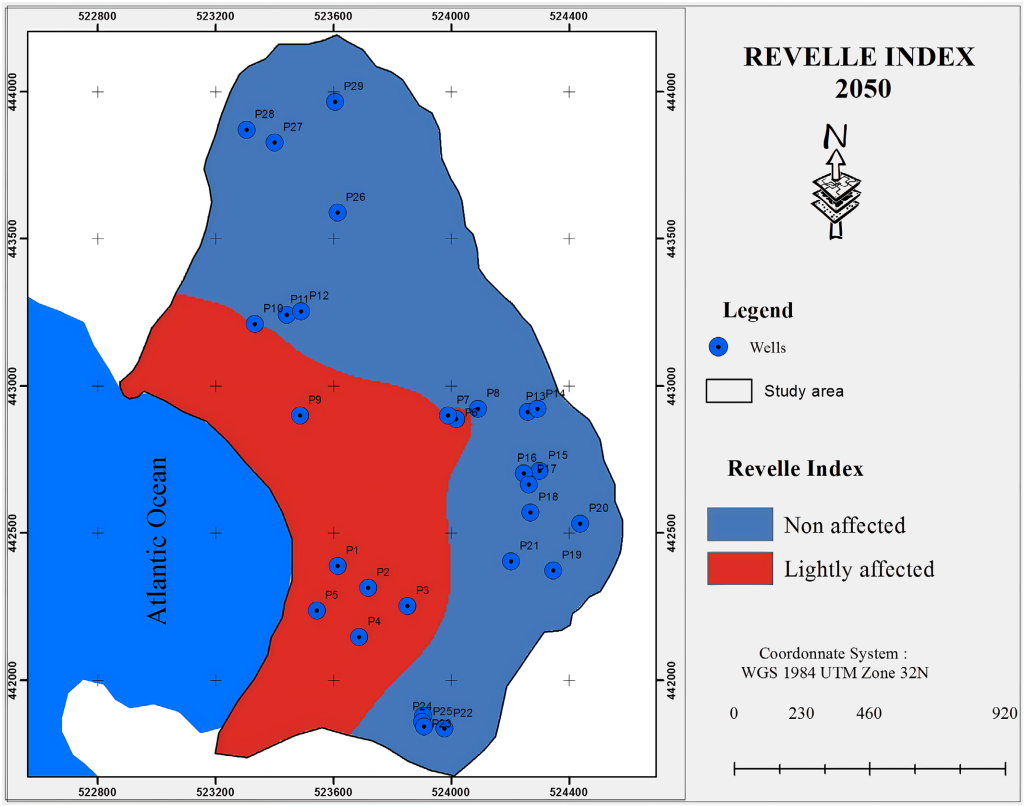

Figure 5. Spatial variation of Revelle index 2050.

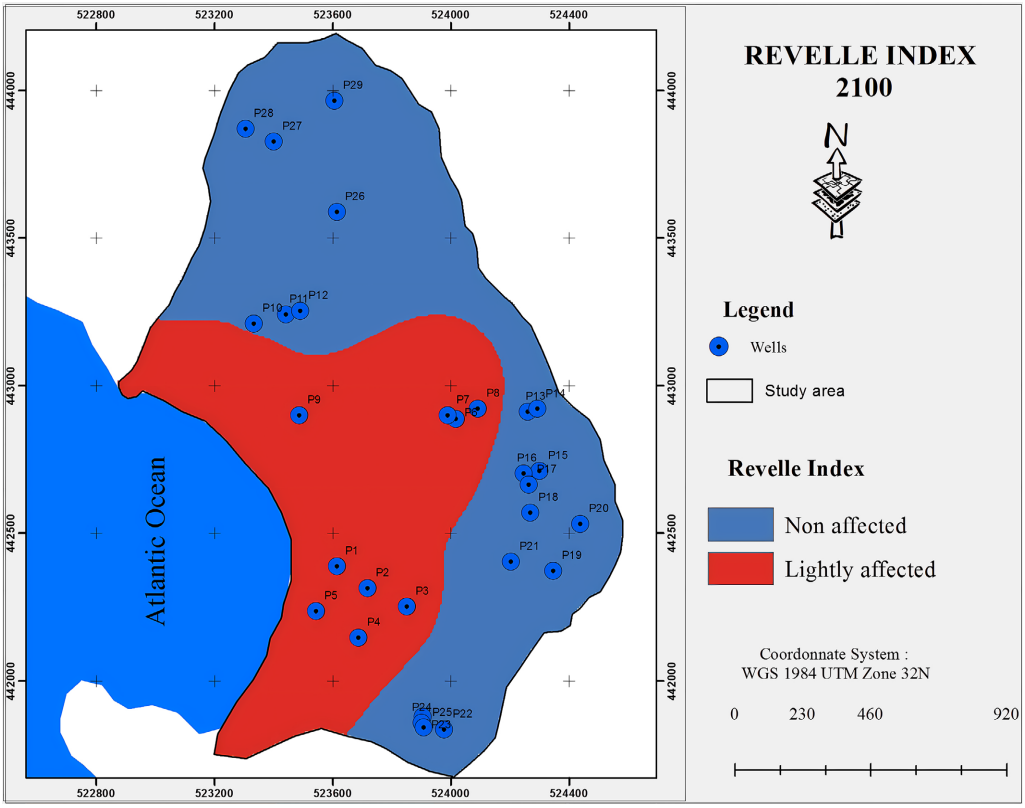

Figure 6. Spatial variation of the Revelle index 2100.

3.2. The Current Spatial Variability (SP) and SP of Water Quality Due to Sea Level Rise Resulting from Climate Change Using WQI

The suitability of groundwater quality for drinking purposes in the study area was determined using [13] guidelines. The computed Water Quality Index (WQI) ranged from 28 to 115 as indicated in Table 6. From the table, chloride and electrical conductivity are primary drivers of WQI values, as they are strong indicators of a water source's overall solute content and salinity, and are linked to negative effects on human health. This result is similar to that of [38], when they studied the relationship between chloride concentration and electrical conductivity in groundwater and its estimation from vertical electrical soundings (VESs) in Guasave, Sinaloa, Mexico.

Table 6. Water Quality Index in the study area for 2018, 2050, 2100.

Transects	Wells	X	Y	WQI 2018	WQI 2050	WQI 2100
T1	P1	523,612	442,388	84	84	84
T1	P2	523,716	442,314	108	108	108
T1	P3	523,850	442,252	93	93	93
T1	P4	523,686	442,146	115	115	115
T1	P5	523,541	442,236	114	114	114
T1	P9	523,484	442,900	73	73	73
T1	P10	523,331	443,210	67	67	67
T1	P11	523,439	443,241	84	84	84
T2	P6	524,016	442,888	72	77	77
T2	P7	523,988	442,900	96	102	102
T2	P8	524,090	442,922	97	100	100
T2	P12	523,488	443,253	69	86	86
T2	P15	524,299	442,711	28	28	49
T2	P16	524,245	442,703	29	29	40
T2	P17	524,262	442,665	35	35	44
T2	P18	524,267	442,570	57	57	57
T2	P19	524,346	442,372	28	28	28
T2	P21	524,202	442,404	42	42	42
T2	P26	523,612	443,589	44	44	44
T2	P27	523,399	443,827	64	64	64
T2	P28	523,303	443,870	53	53	53
T2	P29	523,604	443,966	42	42	42

Continued

T2	P30	523,634	443,866	48	48	48
T3	P13	524,259	442,912	51	51	51
T3	P14	524,291	442,921	48	48	48
T3	P20	524,437	442,532	41	41	41
T3	P22	523,976	441,835	40	40	40
T3	P23	523,903	441,878	40	40	40
T3	P24	523,899	441,857	44	44	44
T3	P25	523,907	441,841	43	43	43
			Min	28	28	28
			Max	115	115	115
			Mean	62	63	64
			Standard devia	26.41	27.27	25.91

The spatial distribution of water types in the study period is presented in Figure 7. Figure 8 and Figure 9 show the spatial distribution based on projected sea level rise resulting from climate change. The EC, pH, TDS, Cl^-, and HCO_3^- all contributed to the WQI values. However, values of chloride and electrical conductivity were the main parameters responsible for the high values of WQI. In some locations, the TDS also significantly increased the WQI.

The area covered by various water types is calculated from the WQI maps and given in Table 7. About 34.4% of the gw is currently considered to be good for drinking, while 65.6% is either poor, very poor, or unsuitable for drinking. As the years go by, based on projected sea level rise due to climate change, the amount of seawater intrusion is set to increase if there are no mitigating measures. The proportion of gw considered to be of good quality is therefore projected to reduce as more gw becomes polluted by seawater. From Table 6, in 2050, the proportion of the groundwater considered to be good for drinking will reduce to 26.92%, and down to 17.86% in 2010. Hot spots that require urgent attention are locations of wells P_2, P_3, P_4, and P_5.

Table 7. Area covered by different water types.

Groundwater quality	2018 (ha)	2050 (ha)	2100 (ha)
Unsuitable for drinking	16.38 (6.79%)	42.78 (17.73%)	60.65 (25.13%)
Very poor	60.63 (25.12%)	70.68 (29.29%)	68.55 (28.41%)
Poor	81.30 (33.69%)	62.90 (26.06%)	69.02 (28.60%)
Good	83.01 (34.40%)	64.96 (26.92%)	43.10 (17.86%)
Total	241.32 (100%)	241.32 (100%)	241.32 (100%)

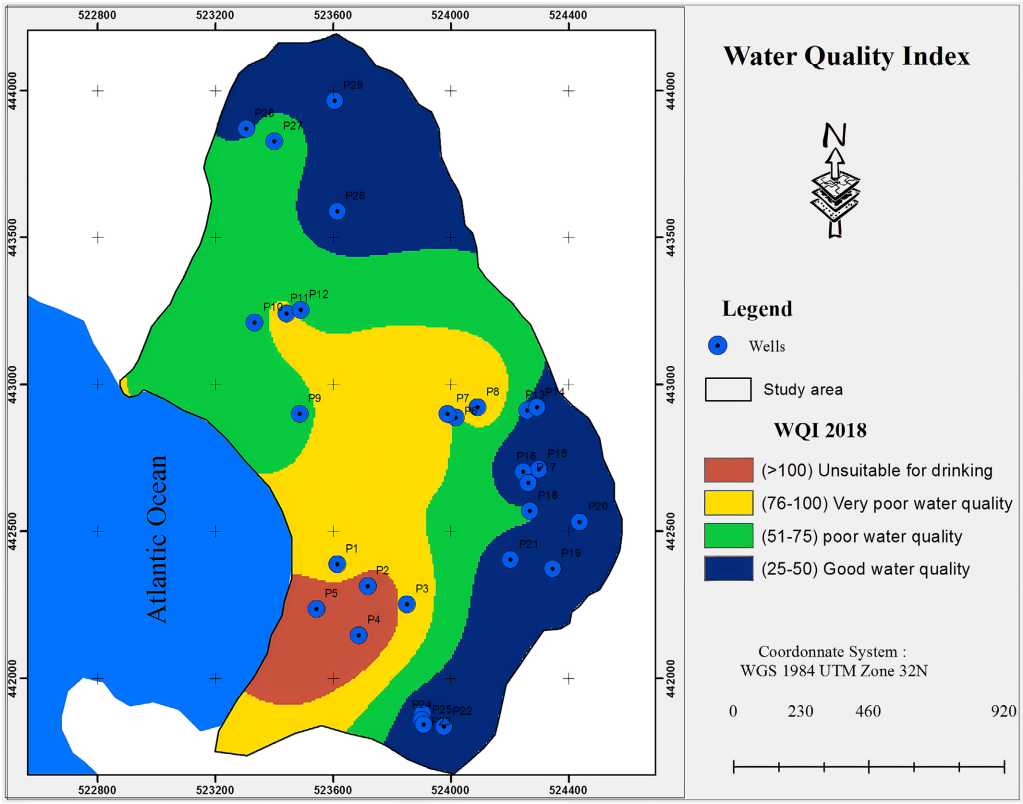

Figure 7. Spatial variation of the Water Quality Index in 2018.

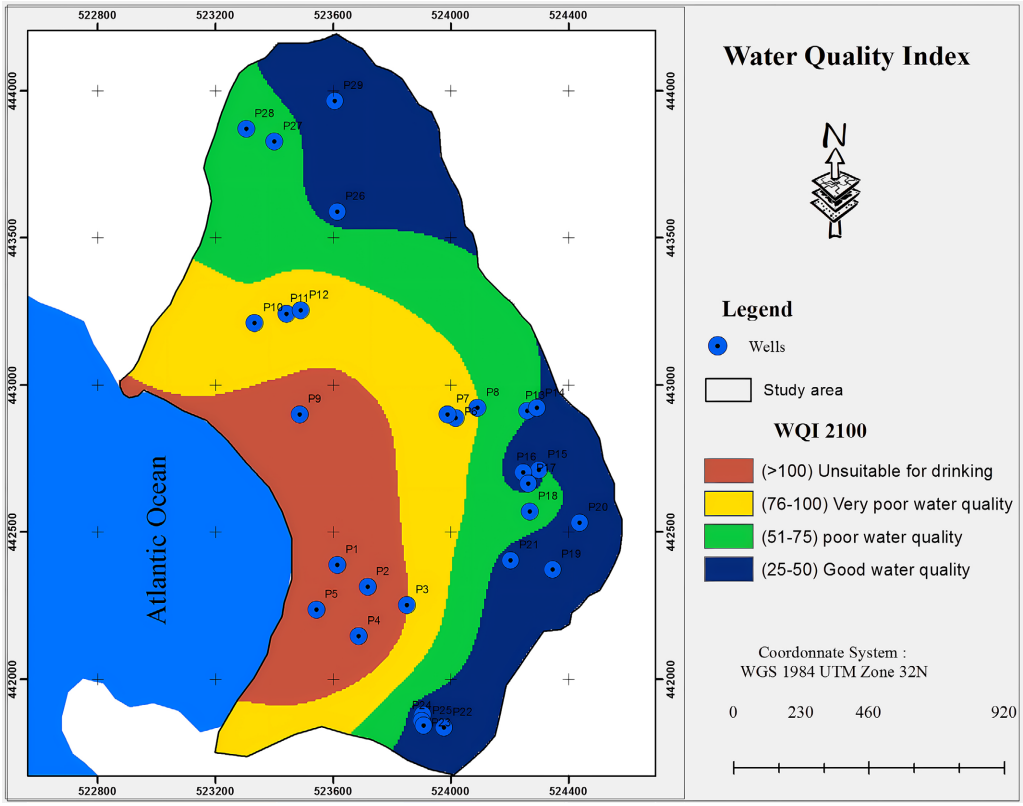

Figure 8. Spatial variation of WQI in 2050 based on a projected sea level rise of 0.32 m.

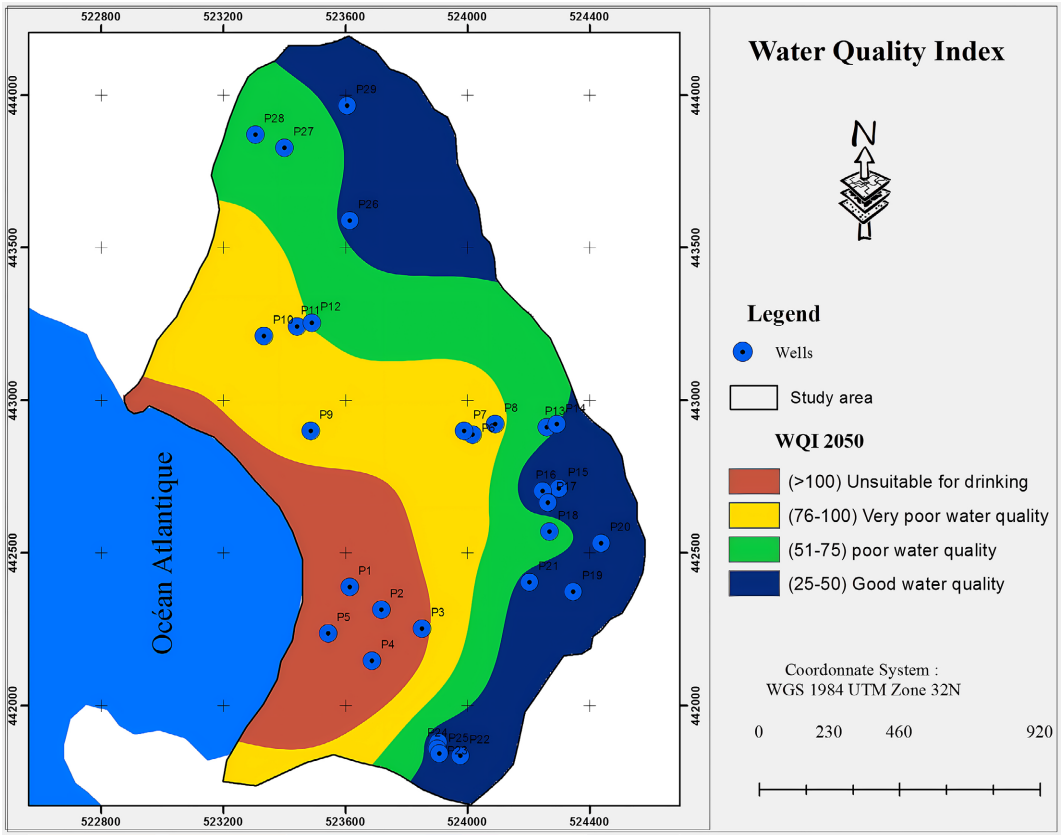

Figure 9. Spatial variation of WQI in 2100 based on a projected sea level rise of 0.82 m.

4. Conclusions

Based on the methodology used in this study and the results obtained, it can be concluded that:

1) About 23% of the groundwater resources in the study area are presently slightly polluted by seawater intrusion. By 2050, this is projected to increase to 30.8% and to 42.31% in 2100 due to increased seawater intrusion resulting from sea level rise because of climate change.

2) Groundwater contamination by seawater intrusion is a major concern for the freshwater supply in the study area, especially around locations of wells P_2, P_3, P_4, and P_5.

3) The Water Quality Index (WQI) ranged from 28 to 115. The EC, pH, TDS, Cl^-, and HCO_3^- all contributed to the WQI values. However, values of chloride and electrical conductivity were the main parameters for the high values of WQI.

4) About 34.4% of the groundwater resources in the study area are currently considered to be good for drinking, while 65.6% are either poor, very poor, or unsuitable for drinking.

5) The proportion of groundwater considered to be of good quality in Limbe is projected to decrease as more groundwater becomes polluted by seawater. In 2050, the proportion of groundwater considered to be good for drinking will decrease to 26.92%, and down to 17.86% in 2100. Hot spots that require urgent at-

tention are locations of wells P_2, P_3, P_4, and P_5.

In light of the findings of this study, some low and "no-regret" investments that yield benefits even in the absence of climate change should be carried out to minimize the impact of saline intrusion on the quality of gw in the study area. These include shoreline vegetation and forest planting, mangrove restoration and replanting at the mouth of the Njenguele River, and seagrass replanting. There is also a need for strengthening the ongoing plans for integrated coastal zone management.

Acknowledgements

The authors are most grateful to the water utility company in Limbe for their collaboration in this study. Special thanks to all those who participated in the collection of data, in the laboratory analyses, and to the population of the study area for their support.

Conflicts of Interest

The authors declare no conflicts of interest regarding the publication of this paper.

References

[1] Rejith, P.G., Jeeva, S.P., Vijith, H., Sowmya, M. and Mohamed, A.A.H. (2009) Determination of Groundwater Quality Index of a Highland Village of Kerala (India) Using Geographical Information System. *Journal of Environmental Health*, **71**, 51-58.

[2] Patwardhan, A. (2003) Changing Status of Urban Water Bodies and Associated Health Concerns in Pune, India. *Proceedings of the* 3*rd International Conference on Environment and Health*, Chennai, 15-17 December 2003, 339-345.

[3] Motchemien, R. and Fonteh, M.F. (2020) The Impact of Sea Water Intrusion on the Spatial Variability of the Physical and Chemical Properties of Groundwater in Limbe-Cameroon. *African Journal of Environmental Science and Technology*, **14**, 92-103. https://doi.org/10.5897/ajest2020.2828

[4] Douglas, B.C. (1997) Global Sea Level Rise: A Redetermination. *Surveys in Geophysics*, **18**, 279-292.

[5] Intergovernmental Panel on Climate Change (IPCC) (2007) Climate Change 2007. Cambridge University Press.

[6] Bates, B., Kundzewicz, Z.W., Wu, S. and Palutikof, J. (2008) Climate Change and Water. Technical Paper of the Intergovernmental Panel on Climate Change. IPCC Secretariat.

[7] Nicholls, R.J. and Cazenave, A. (2010) Sea-Level Rise and Its Impact on Coastal Zones. *Science*, **328**, 1517-1520. https://doi.org/10.1126/science.1185782

[8] Werner, A.D. and Simmons, C.T. (2009) Impact of Sea-Level Rise on Sea Water Intrusion in Coastal Aquifers. *Groundwater*, **47**, 197-204. https://doi.org/10.1111/j.1745-6584.2008.00535.x

[9] Lacombe, P.J. and Carleton, G.B. (1992) Carleton Salt Water Intrusion into Fresh Ground-Water Supplies, Southern Cape May County. *Proceedings of the National Symposium on the Future Availability of Groundwater Resources*, New Jersey, 12-15 April 1992, 287-298.

[10] Li, H.L. and Jiao, J.J. (2003) Tide-Induced Seawater-Groundwater Circulation in a Multi-Layered Coastal Leaky Aquifer System. *Journal of Hydrology*, **274**, 211-224. https://doi.org/10.1016/s002-1694(02)00413-4

[11] Feseker, T. (2007) Numerical Studies on Saltwater Intrusion in a Coastal Aquifer in Northwestern Germany. *Hydrogeology Journal*, **15**, 267-279. https://doi.org/10.1007/s10040-006-0151-z

[12] Esteller, M.V., Rodríguez, R., Cardona, A. and Padilla-Sánchez, L. (2012) Evaluation of Hydrochemical Changes Due to Intensive Aquifer Exploitation: Case Studies from Mexico. *Environmental Monitoring and Assessment*, **184**, 5725-5741. https://doi.org/10.1007/s10661-011-2376-0

[13] World Health Organization (WHO) (2006) Guidelines for Drinking Water Quality. WHO.

[14] Sargaonkarm, A. and Deshpande, V. (2003) Development of an Overall Index of Pollution for Surface Water Based on a General Classification Scheme in Indian Context. *Environmental Monitoring and Assessment*, **89**, 43-67. https://doi.org/10.1023/a:1025886025137

[15] Shah, M.C., Shilpkar, P.G. and Acharya, P.B. (2008) Groundwater Quality of Gandhinagar Taluka, Gujarat, India. *Journal of Chemistry*, **5**, 435-446. https://doi.org/10.1155/2008/481694

[16] Zaharin, A.A., Abdullah, M.H. and Praveena, S.M. (2009) Evolution of Groundwater Chemistry in the Shallow Aquifer of a Small Tropical Island in Sabah. Malaysia. *Sains Malaysiana*, **38**, 805-812.

[17] Chachadi, A.G. and Lobo-Ferreira, J.P. (2001) Sea Water Intrusion Vulnerability Mapping of Aquifers Using GALDIT Method. *Proceedings of Workshop on Modelling in Hydro-Geology at Anna University*, Chennai, 3-7 December 2001, 143-156.

[18] Akoteyon, I.S. (2013) Evaluation of Groundwater Quality Using Water Quality Indices in Parts of Lagos-Nigeria. *Journal of Environmental Geography*, **6**, 29-36. https://doi.org/10.2478/v10326-012-0004-2

[19] Vasanthavigar, M., Srinivasamoorthy, K., Vijayaragavan, K., Rajiv Ganthi, R., Chidambaram, S., Anandhan, P., *et al.* (2010) Application of Water Quality Index for Groundwater Quality Assessment: Thirumanimuttar Sub-Basin, Tamilnadu, India. *Environmental Monitoring and Assessment*, **171**, 595-609. https://doi.org/10.1007/s10661-009-1302-1

[20] Ramakrishnaiah, C.R., Sadashivaiah, C. and Ranganna, G. (2009) Assessment of Water Quality Index for the Groundwater in Tumkur Taluk, Karnataka State, India. *Journal of Chemistry*, **6**, 523-530. https://doi.org/10.1155/2009/757424

[21] Rao, S.G. and Nageswararao, G. (2013) Assessment of Groundwater Quality Using Water Quality Index. *Archives of Environmental Science*, **7**, 1-5.

[22] Sahu, P. and Sikdar, P.K. (2008) Use of Water Quality Indices to Verify the Impact of Cordoba City (Argentina) on Suquy'a River. *Geology Journal*, **55**, 823-835.

[23] Institut National de Statistiques (INS) (2013) Annuaire statistique du Cameroun, Yaoundé. INS.

[24] Njabe, R.K. and Fobang, R. (2006) Illustrated Physical Geography and Map Reading for Cameroon. 3rd Edition, Sunway Publisher.

[25] Ndille, R. and Belle, J.A. (2014) Managing the Limbe Floods: Considerations for Disaster Risk Reduction in Cameroon. *International Journal of Disaster Risk Science*, **5**, 147-156. https://doi.org/10.1007/s13753-014-0019-0

[26] Nwankiti, O.C. (1983) Man and His Environment. Longman Group.

[27] Buh, W.G. (2009) Geographic Information Systems-Based Demarcation of Risk Zones: The Case of the Limbe Sub-Division—Cameroon. *Journal of Disaster Risk Studies*, **1**, 600-617.

[28] Suh, C.E., Ayonghe, S.N., Sparks, R.S.J., Annen, C., Fitton, J.G., Nana, R., *et al.* (2003) The 1999 and 2000 Eruptions of Mount Cameroon: Eruption Behaviour and Petrochemistry of Lava. *Bulletin of Volcanology*, **65**, 267-281. https://doi.org/10.1007/s00445-002-0257-7

[29] Fombe, L.F. and Molombe, J.M. (2015) Hydro-Geomorphological Implications of Uncontrolled Settlements in Limbe, Cameroon. *International Review of Social Sciences*, **4**, 169-183.

[30] Diko, M.L, Ekosse, G.E., Ayonghe, S.N. and Ntasin, E.B. (2012) Physical and Geotechnical Characterization of Unconsolidated Sediments Associated with the 2005 Mbonjo Landslide, Limbe, Cameroon. *International Journal of Physical Sciences*, **7**, 2784-2790.

[31] Longe, E.O. (2011) Groundwater Resources Potential in the Coastal Plain Sands Aquifers, Lagos, Nigeria. *Research Journal of Environmental and Earth Sciences*, **3**, 1-7.

[32] Howell, D.C. (1999) Méthodes statistiques en sciences humaines. De Boeck Université.

[33] American Public Health Association (APHA) (1998) Standard Methods for the Examination of Water and Wastewater. 20th Edition, APHA.

[34] Revelle, R. (1941) Criteria for Recognition of Sea Water in Groundwater. *Transactions of American Geophysical Union*, **22**, 593-597.

[35] Chatterji, C. and Raziuddin, M. (2002) Determination of Water Quality Index (WQI) of a Degraded River in Asanol Industrial area, Raniganj, Burdwan, West Bengal. *Nature, Environment and Pollution Technology Journal*, **2**, 181-189.

[36] Dörfliger, N., Schomburgk, S., Bouzit, M., Petit, V., Caballero, Y., Durst, P., Douez, O., Chatelier, M., Croiset, N. and Surdyk, N. (2011) Montée du niveau marin induite par le changement climatique: Conséquences sur l'intrusion saline dans les aquifères côtiers en Métropole. BRGM.

[37] Chandra, S., Singh, A. and Tomar, P.K. (2012) Assessment of Water Quality Values in Porur Lake Chennai, Hussain Sagar Hyderabad and Vihar Lake Mumbai, India. *Chemical Science Transactions*, **1**, 508-515. https://doi.org/10.7598/cst2012.169

[38] Peinado-Guevara, H., Green-Ruíz, C., Herrera-Barrientos, J., Escolero-Fuentes, O., Delgado-Rodríguez, O., Belmonte-Jiménez, S., *et al.* (2012) Relationship between Chloride Concentration and Electrical Conductivity in Groundwater and Its Estimation from Vertical Electrical Soundings (VESs) in Guasave, Sinaloa, Mexico. *Ciencia e investigación agraria*, **39**, 229-239. https://doi.org/10.4067/s0718-16202012000100020